

# Organic Beam Epitaxy Using Controlled PMDA–ODA Coupling Reactions on Cu{110}

S. Haq and N. V. Richardson\*

Surface Science Research Centre, The University of Liverpool, Liverpool L69 3BX, U.K.

Received: December 30, 1998; In Final Form: April 8, 1999

Reflection–absorption infrared spectroscopy (RAIRS) has been used to study in detail, as a function of temperature and coverage, the interaction of pyromellitic dianhydride (PMDA) and 4,4-oxydianiline (ODA) on the clean and oxygen-precovered Cu{110} surfaces. On the clean surface, both molecules show coverage-dependent reorientation from flat lying to upright species. The adsorption of PMDA on the clean surface leads to a ring-opening reaction of one of the anhydride group to produce a species with both carbonyl and carboxylate groups. The carbonyl group is lost into the gas phase above 350 K, with the resulting anhydride species bonded to the surface via the carboxylate group. The presence of preadsorbed oxygen also leads to the reaction of one of the anhydride groups, although in this case a dicarboxylate (phthalate) anhydride species is produced. The condensation reaction of 4,4-oxydianiline with the two PMDA-derived species has also been studied. It is shown that the PMDA–ODA oligomer can be grown layer by layer using controlled imide coupling reactions. The growth is monitored by IR spectroscopy.

## 1. Introduction

The growth of thin polymer films under well-defined and controlled conditions is of significant technological importance, especially in the microelectronics industry where they are often used as packaging materials and as dielectric interlayers. In particular, polyimide films are being increasingly used for such applications due to their low dielectric constant as well as their good chemical resistance and thermal stability.<sup>1</sup> The physical performance of these films is dependent on both the adhesion at the interface and their uniformity. The technological importance of thin polyimide films has inevitably led to a large number of studies documenting their fabrication, chemical and structural properties.<sup>1</sup>

Polyimide films can be prepared in one of two ways. The first, industrially more common, is by spin coating with a solution of polyamic acid onto the desired substrate and subsequently heating to produce the polyimide.<sup>2</sup> The second is by in-situ vapor codeposition of the individual monomers, pyromellitic dianhydride (PMDA) and oxydianiline (ODA), which react to form the polyamic acid which is then heated to produce the polyimide.<sup>3</sup> The structures of PMDA and ODA are included in Figures 6 and 8, respectively. Clearly vacuum codeposition represents a much cleaner and controllable process. Furthermore, this method of preparation has allowed a detailed study to be undertaken of the interfacial chemistry. It is crucial to obtain the correct deposition stoichiometry to minimise unwanted side reactions leading to isoimide linkages.

Recently, in an extension of the vapor deposition method, it has been shown that the growth of oriented oligomides might be achieved by the sequential adsorption and reaction of alternating dianhydrides and diamines brought to a metal surface by vapor deposition in ultra high vacuum.<sup>4–7</sup> To exploit this controlled organic thin film growth process, it is essential to fully characterize the initial organic/metal interface, an initial

dianhydride adsorption step leading to a strong surface bond, with the second anhydride group directed away from the surface ready for reaction with an amine. Therefore, we studied a series of related molecules, including phthalic anhydride, reacting with copper as a function of temperature and coverage, which has allowed us to understand the structural and chemical aspects of the surface bonding interaction of an anhydride group in precise detail.<sup>8,9</sup> As a consequence, it is now well established that the anhydride group reacts with the metal surface to produce a strong surface carboxylate species. This forms a basis for the understanding the adsorption of PMDA, a more complex dianhydride, on a metal surface and its subsequent reaction with an amine to form the oligomer/polymer.

The majority of related studies to date have concentrated on the formation of the precursor amic acid: either by coadsorption of PMDA and ODA to form a mixed multilayer<sup>10,11</sup> or by simultaneous vapor codeposition,<sup>12–15</sup> followed by thermally induced imidization. Both these methods lead to the formation of polymer chains of random orientation and length. In this paper, we develop on our previous IR and HREELS work in which the interaction of related molecules was investigated in detail and focus on the extension of the polymer chain length using a layer by layer growth process. The adsorption of the individual molecules on the clean surface is studied as well as the condensation reaction. Since preadsorbed oxygen is able to influence the anhydride copper reaction, we have investigated its ability to improve the growth characteristics.

After an experimental section, in section 3 we first characterize the adsorption of PMDA on clean and oxygen predosed Cu(110) as a function of coverage and temperature. In section 4, we briefly describe the behavior of ODA on Cu(110). In section 5 the coupling reactions of PMDA and ODA are presented and discussed before a final summary in section 6.

## 2. Experimental Section

The investigations were conducted in a UHV chamber equipped with facilities for cleaning (Ar<sup>+</sup> gun) and characterization of single-crystal surfaces, including low-energy electron

\* Corresponding author. Present address: School of Chemistry, North Haugh, University of St. Andrews, St. Andrews, Fife, Scotland, KY16 9ST, U.K. E-mail: nvr@st-and.ac.uk.

diffraction (LEED), mass spectrometric TPD, and reflection-absorption FTIR. The chamber is interfaced to a commercial FTIR spectrometer (Mattson Galaxy) via differentially pumped KBr windows and a narrow band MCT detector permits access to the spectral range 650–4000  $\text{cm}^{-1}$ . Spectra were typically measured at a resolution of 4  $\text{cm}^{-1}$  with co-addition of 256 or 400 scans, and are displayed as the ratio ( $\Delta R/R$ ) relative to the clean surface spectrum.

The copper single crystal was mechanically cut and polished to within  $0.5^\circ$  of the  $\{110\}$  face then cleaned, in situ, using cycles of  $\text{Ar}^+$  bombardment (500 eV, 8  $\mu\text{A}$ ) and annealing (750 K). The pyromellitic dianhydride (PMDA) and 4,4-oxydianiline (ODA) (Aldrich Chemicals) were dosed from a specially constructed dosing manifold. This consisted of a small, electrically heated, pyrex glass tube mounted on a flange on a four-way cross, which is separated from the main chamber by a gate valve and differentially pumped with a turbomolecular pump. The distance of the glass tube to the crystal is  $\sim 25$  cm. With this arrangement the adsorption rate could be precisely controlled by varying the temperature of the glass tube, which is measured with a K-type thermocouple attached to the end of the tube. The chamber base pressure was  $1 \times 10^{-10}$  mbar and during dosing rose to a maximum of  $\sim 5 \times 10^{-9}$  mbar. Recovery of the vacuum after dosing is slow, making precise estimates of sample exposure difficult. The purity of the compounds was confirmed by mass spectrometry upon admission to the chamber.

### 3. Adsorption of Pyromellitic Dianhydride

**3.1. Adsorption of PMDA on Clean Cu $\{110\}$  95 and 200 K.** As there are a large number of vibrational modes associated with the PMDA molecule, it is useful to establish their frequencies and relative intensities on the Cu $\{110\}$  surface at low temperature, where we might anticipate the predominance of undissociated PMDA species. Figure 1 shows the IR spectra measured as a function of increasing coverage at 95 K and the subsequent changes with thermal evolution. Even at this low temperature, however, the small bands that are initially observed at 1744 and 1687  $\text{cm}^{-1}$  do not correlate with those of intact PMDA. This indicates some modification of the incoming molecules upon adsorption in the monolayer regime. However, the frequencies and relative intensities of the vibrational modes for the intact PMDA molecules can be determined from the multilayer spectra obtained at the higher coverages; these are listed and assigned in Table 1. As expected, the most intense bands are those associated with the stretching and bending motions of the anhydride groups. The frequencies and relative intensities of the modes in the multilayer compare well with those of the PMDA/Pt $\{111\}$  system,<sup>16</sup> although in that system a change in the relative intensities was seen due to a transition from an amorphous to crystalline phase at 273 K. On Cu(110), at this temperature desorption of the multilayers dominates instead, presumably due to lesser thickness of the multilayer used.

The development of the small bands with increasing coverage in the monolayer regime at low temperature are more clearly shown in Figure 2, with adsorption at 200 K. Initially, two bands appear at 1718 and 1266  $\text{cm}^{-1}$ . Both of these maximize their intensities with increasing coverage and remain constant thereafter. The band at 1718  $\text{cm}^{-1}$  shifts to 1747  $\text{cm}^{-1}$  with increasing coverage. In the initial stages of adsorption a small broad band at 1630  $\text{cm}^{-1}$  is also seen, although this disappears with increasing coverage. Spectra c and d show the start of two distinct changes in the spectra. First, spectrum c shows the appearance of modes at 1862, 918, and 718  $\text{cm}^{-1}$ , and subsequently spectrum d shows strong additional bands at 1810,

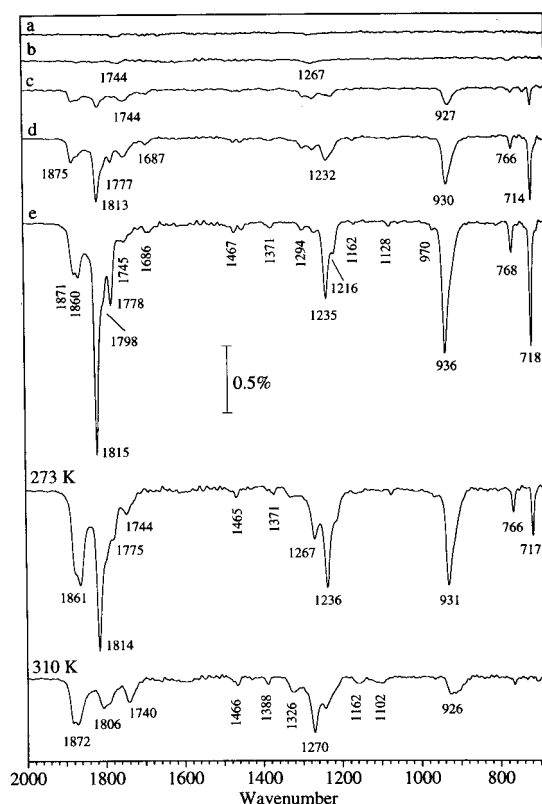


**Figure 1.** IR spectra of PMDA adsorption on clean Cu $\{110\}$  with increasing coverage at 95 K and heating the resulting overlayer to 273 and 310 K. Spectra a–e were recorded during a  $5 \times 10^{-9}$  mbar continual dose.

**TABLE 1: Normal Modes of Vibration for PMDA<sup>a</sup>**

mode description		solid <sup>a</sup>	Cu $\{110\}$		
			multilayer	clean	(2 $\times$ 1)O
$\nu_1$	$A_g$	$\nu(\text{C-H})$	3106 s		
$\nu_{28}$	$B_{1u}$	$\nu(\text{C-H})$	3056 m		
$\nu_2$	$A_g$	$\nu(\text{C=O})$	1872 vs	1871	1871
$\nu_{36}$	$B_{2u}$	$\nu(\text{C=O})$	1854 vs	1860	
$\nu_{17}$	$B_{3g}$	$\nu(\text{C=O})$	1790 vs	1815	1798
$\nu_{29}$	$B_{1u}$	$\nu(\text{C=O})$	1775 vs	1778	1808
$\nu_3$	$A_g$	$\nu(\text{C-C})$	1627 vs		
$\nu_{18}$	$B_{3g}$	$\nu(\text{C-C})$	1574 w		
$\nu_{37}$	$B_{2u}$	$\nu(\text{C-C})$	1464 s	1467	1468
$\nu_{30}$	$B_{1u}$	$\nu(\text{C-C})$	1373 m	1371	1472
$\nu_{31}$	$B_{1u}$	$\nu(\text{C-C})$	1306	1294	1317
$\nu_{38}$	$B_{2u}$	$\nu(\text{C-O})$	1276 vs	1235	1327
$\nu_{20}$	$B_{3g}$	$\delta(\text{C-H})$	1262 w	1235	1267
$\nu_{39}$	$B_{2u}$	$\nu(\text{C-C})$	1238 vs	1216	1275
$\nu_5$	$A_g$	$\nu(\text{C-C})$	1132 w	1162	1227
$\nu_{40}$	$B_{2u}$	$\nu(\text{C-C})$	1119 w	1128	1153
$\nu_{41}$	$B_{2u}$	$\delta(\text{C-H})$	1075 m	1102	1161
$\nu_{21}$	$B_{3g}$	$\nu(\text{C-O})$	937 vw	1107	1107
$\nu_{32}$	$B_{1u}$	$\nu(\text{C-O})$	924 vs	936	908
$\nu_{13}$	$B_{3u}$	$\delta(\text{C-H})$	904 w		912
$\nu_{33}$	$B_{1u}$	$\delta(\text{CCC})$	767 vs		
$\nu_{14}$	$B_{2g}$	$\gamma(\text{C=O})$	766 m	766	
$\nu_6$	$A_g$	$\nu(\text{C-C})$	755 vs		730
$\nu_{45}$	$B_{3u}$	$\gamma(\text{C=O})$	710 vs	718	731

<sup>a</sup> After Hase et al.<sup>25</sup>

1234, 929, and 716  $\text{cm}^{-1}$ . These latter modes continue to grow with increasing exposure. The frequencies and intensities of these modes are similar to those observed for the intact molecules as seen in the multilayer spectra, indicating the start of the formation of a second layer. It is difficult to establish the exact point this starts as these bands could also arise from intact molecules within the first layer. However, our primary

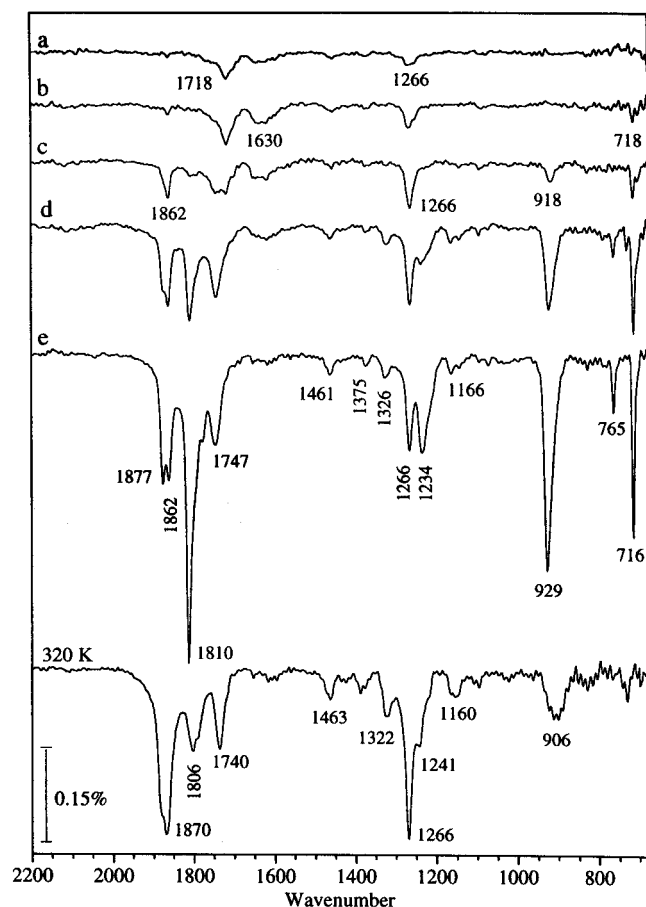


**Figure 2.** IR spectra of PMDA adsorption on clean Cu{110} with increasing coverage at 200 K, a–e, and heating the resulting overlayer to 320 K.

interest is the monolayer, and thus warming the surface to 320 K leaves a saturated surface after the desorption of the molecules which are not strongly chemisorbed.

### 3.2. Adsorption of PMDA on Clean Cu{110} 300 K.

Adsorption at room temperature leads to a variation in the relative intensities of the modes observed at ~1640 and 1736 cm⁻¹ as shown in spectra a–d of Figure 3. Here distinct changes can be seen with increasing coverage; at low coverage two bands are observed at 1640 and 1263 cm⁻¹. With increasing coverage the former completely attenuates as strong bands appear at 1871, 1804, 1736, 1267, and 922 cm⁻¹. On warming this surface to above 370 K, spectrum e, there is yet another change in the IR spectrum with the complete attenuation of the mode at 1736 cm⁻¹. The loss of this mode is accompanied by the evolution of CO into the gas phase as shown in Figure 4.

**3.3. Adsorption of PMDA on (2×1)O/Cu{110} 300 K.** The IR spectra from the adsorption of PMDA on a (2×1) oxygen-precovered surface at 300 K are shown in Figure 5, again as a function of increasing coverage. On this surface, there is no change in the relative intensities of any of the bands, and the intensity of all the bands increases steadily with increasing coverage. The characteristic anhydride modes are observed at 1871, 1808, 1275, and 912 cm⁻¹. Additional modes are seen at 1553, 1424, and 846 cm⁻¹, which we do not observe for the clean surface adsorption or the multilayer spectrum which represent the parent molecule. Unlike the clean surface, no mode was observed at 1736 cm⁻¹ and no change was observed in spectra on warming this surface to above 370 K. All the modes are listed and assigned in Table 1. An additional point of note is that the absolute intensity of the modes for the clean and

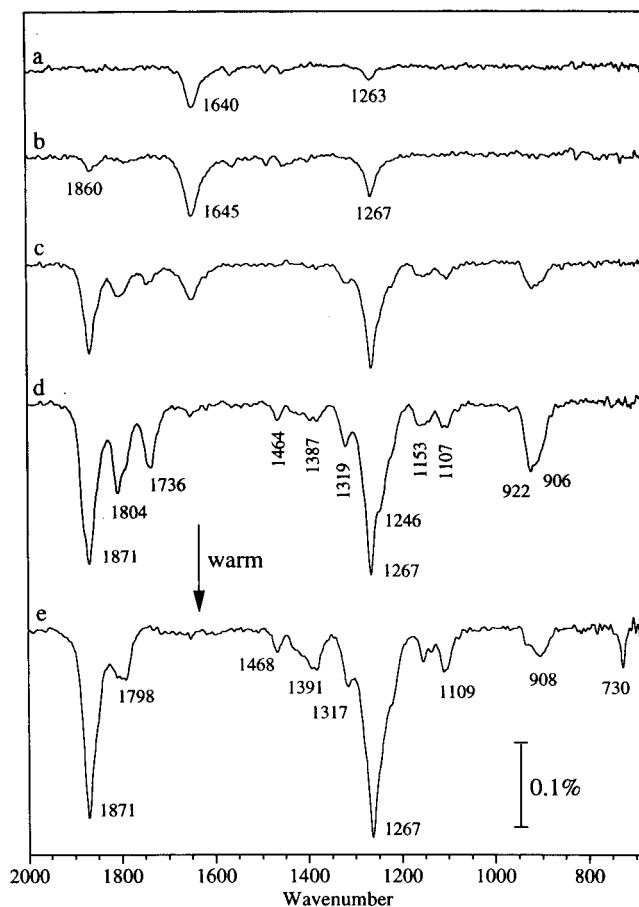


**Figure 3.** IR spectra of PMDA adsorption on clean Cu{110} with increasing coverage at 300 K, a–d. Spectrum e was obtained after heating the overlayer to 370 K.

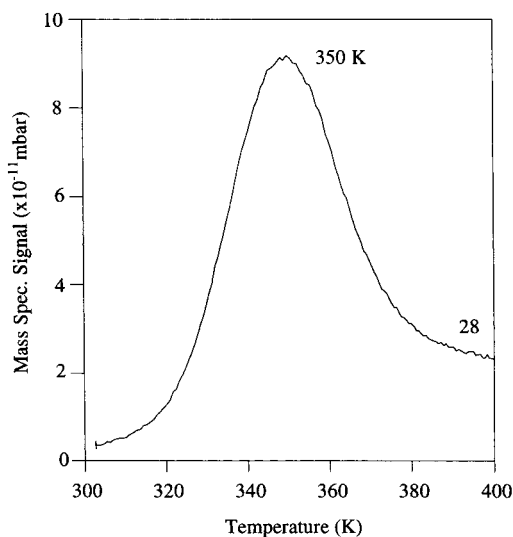


**Figure 4.** TPD spectrum showing evolution of CO (mass 28) after saturation exposure of PMDA on clean Cu{110} at 300 K.

oxygen-precovered saturated surfaces differ by a factor of approximately 4, with the latter more intense.

**3.4. Discussion of PMDA Adsorption.** The isolated PMDA molecule has a quasi-planar structure, close to  $D_{2h}$  symmetry.<sup>17</sup> The strongest dipole active modes are associated with the stretching and bending modes of the anhydride groups. The symmetric ( $b_{2u}$ ) and asymmetric modes ( $b_{1u}$ ) of the ring C–O–C stretching vibrations are found at 1276 and 924 cm⁻¹, respectively. The corresponding modes of the anhydride car-

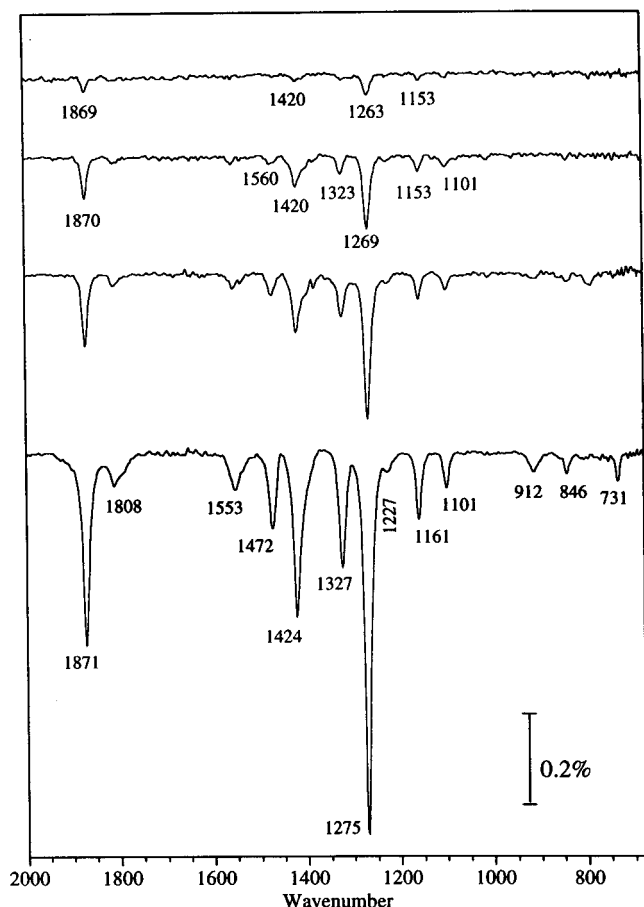


**Figure 5.** IR spectra of PMDA adsorption on (2×1)O/Cu{110} with increasing coverage at 300 K.

bonyl groups are at 1854 and 1775  $\text{cm}^{-1}$ , respectively. In each of these pairs, the symmetric modes at the higher frequency involves a dynamic dipole in the molecular plane parallel to the long  $C_2$  axis of the parent molecule, while the asymmetric mode has a dynamic dipole change in the molecular plane but perpendicular to the long  $C_2$  axis. The most intense out-of-plane mode is the  $\gamma(\text{C}=\text{O})$  at 710  $\text{cm}^{-1}$ . Hahn et al.<sup>16</sup> have shown that in the condensed phase intermolecular coupling of the modes leads to correlation splitting of the IR bands, leading to the observation of four fundamental modes in the 1770–1875  $\text{cm}^{-1}$ , carbonyl stretching region of the anhydride groups. However, we note that the relative intensities do not change as successive layers form, even from the earliest stages of adsorption, which cannot be accounted for solely by correlation splitting and may simply arise from symmetry reduction at the surface. In fact, there are inactive  $\nu(\text{C}=\text{O})$  modes in the isolated species of  $a_g$  and  $b_{3g}$  symmetry at 1870 and 1800  $\text{cm}^{-1}$  respectively, which can become active on adsorption.

In principle, for a homogenous overlayer of planar  $D_{2h}$  molecules, for which the dipole associated with each active mode is parallel to the  $x$ ,  $y$ , or  $z$  axis, it should be relatively straightforward to deduce the orientation at the surface with RAIRS. The PMDA molecule is ideal in this respect in that the modes are relatively strong and the in-plane anhydride carbonyl stretching modes appear as pairs of vibrations of the same symmetry. However, for submonolayer coverages on the clean surface at both low and room temperature, the bands do not correspond to the parent molecule. The results for the adsorption of PMDA on the clean and oxygen-precovered surfaces show strong similarity to those reported previously for phthalic anhydride, therefore we proceed in the analysis by drawing on

this previous work.<sup>8,9</sup> We have shown that the adsorption of phthalic anhydride on Cu{110} leads to a anhydride ring opening reaction. Below 250 K a species with both a carbonyl and carboxylate group was identified, whereas above this temperature the carbonyl group was lost into the gas phase resulting in a benzoate-like species. The orientation of both species showed a complex temperature and coverage dependence; for low coverages the species initially lie flat on the surface and change to an upright geometry with increasing coverage. The loss of a CO unit from the adsorption of PMDA has been observed on a number of surfaces including Ni,<sup>18</sup> Ag,<sup>19,20</sup> Cu,<sup>8,15,21</sup> and Si.<sup>22</sup>

The observation of modes at 1640 and 1740  $\text{cm}^{-1}$ , which do not correlate with any of the modes of PMDA, are taken as an indicator that the PMDA undergoes a similar anhydride ring-opening reaction upon adsorption. Figure 1 indicates that this occurs as low as 95 K. The resulting species is stable to ~330 K and subsequently loses a CO unit, as the TPD spectra clearly show. This, therefore, suggests that the temperature- and coverage-dependent changes in the IR spectra arise from orientational or conformational changes. In keeping with the previous phthalic anhydride studies on this surface, the initial anhydride ring-opening reaction leads to a species with both carbonyl (1740  $\text{cm}^{-1}$ , only seen at high coverages at 300 K) and carboxylate (1640  $\text{cm}^{-1}$ ) groups. The second anhydride group remains unperturbed.<sup>9</sup> The exact nature of this carbonyl group with respect to its conformation and bonding remains uncertain, although we exclude the possibility of formation of an oxycarbonium ion ( $-\text{C}=\text{O}^+$ ) or a ketene ( $=\text{C}=\text{O}$ ) as the frequencies of these are expected above 2100  $\text{cm}^{-1}$ . The vibrational frequencies of a carboxylate group depends on the bonding geometry. Generally for a symmetrically bound carboxylate group, i.e., equivalent C–O bond lengths, two stretching modes are observed;  $\nu_s(\text{OCO})$  and  $\nu_a(\text{OCO})$  between 1400–1440 and 1530–1580  $\text{cm}^{-1}$ , respectively. These frequencies, however, shift if the bond C–O lengths become inequivalent, for instance bonding in a unidentate manner. In the extreme case, the carboxylate group would have a C=O bond and a C–O bond, with the respective frequencies between 1640–1680 and 1200–1300  $\text{cm}^{-1}$ . Therefore, a plausible explanation for the band at 1640  $\text{cm}^{-1}$  is to assign it to a carbonyl stretch of the carboxylate group bonded in a unidentate manner. This assignment conveniently leads to the assignment of the mode observed at 1260  $\text{cm}^{-1}$  to the corresponding C–O stretch. However, the  $\nu_s(\text{COC})$  is also at this frequency but this mode would be accompanied by the  $\nu_s(\text{C}=\text{O})$  of the anhydride at around 1860  $\text{cm}^{-1}$ , which is of the same symmetry. As the latter, or indeed any other anhydride related mode is not observed at low coverage at room temperature but appears, only on increasing coverage, we conclude that the molecule is initially bound in a geometry which makes the anhydride modes IR inactive. One possible geometry, which accounts for these observations, is that the molecules are initially bound with their molecular planes parallel to the surface. However, after the ring opening of one of the anhydride groups the steric repulsion between adjacent carbonyl and carboxylate groups leads to an out-of-plane twisting of the carboxylate group, as shown in Figure 6.

To accommodate increasing coverage, the molecules favor a more upright geometry, which results in a change in bonding of the carboxylate group to become symmetrically bound leading to the disappearance of the  $\nu_a(\text{OCO})$  mode at 1640  $\text{cm}^{-1}$  and the appearance of the  $\nu_s(\text{OCO})$  mode at 1387  $\text{cm}^{-1}$ . This also makes all the other in-plane modes IR active, in particular the



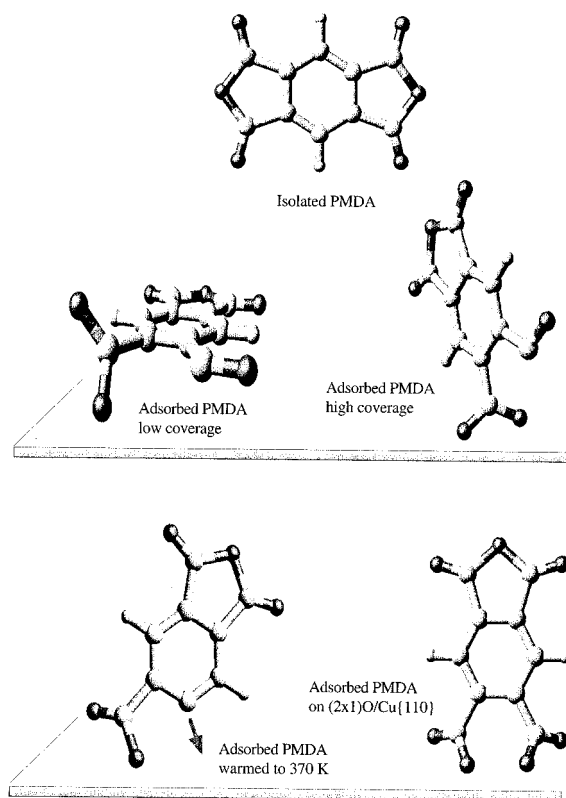


**Figure 6.** Chemical structures and geometry of the PMDA-derived species from adsorption onto the clean and oxygen-precovered Cu{110} surfaces.

modes of the unreacted anhydride group are now observed between 1871–906  $\text{cm}^{-1}$ . The band at 1736  $\text{cm}^{-1}$  is assigned to a carbonyl mode formed after ring-opening reaction of one of the anhydride groups with the Cu{110} surface, as described above. The simultaneous appearance of this latter mode with the modes of the unreacted anhydride group with increasing coverage indicates that these two groups are in the same plane (Figure 6). The assignment of the 1736  $\text{cm}^{-1}$  band to a carbonyl mode is further supported by the IR spectrum taken after the surface is warmed to above 370 K (spectrum e of Figure 3) with the complete attenuation of this mode together with the simultaneous liberation of CO into the gas phase (Figure 4). A major difference between the adsorption of PMDA and PA on Cu{110} is that the evolution of CO into the gas phase is shifted 70 K higher in temperature. The loss of a CO unit from each adsorbed molecule as the surface is warmed to 370 K leaves a species bonded through both the carboxylate group and the  $\alpha$ -carbon of the phenyl ring, as shown in Figure 6. This configuration is consistent with the observation of a relatively larger intensity of the in-phase compared to the out-of-phase carbonyl stretching modes of the anhydride ring as the dipole moment associated with the former modes should be oriented more towards the surface normal. The low-temperature IR spectra are consistent with the anhydride ring-opening reaction, although the evolution of the spectra from low coverage differs from the room temperature spectra. The difference between the spectra may arise from an activation barrier which at low temperature prevents the adsorbed species attaining its optimal conformation.

Previously, we have shown that the adsorption of phthalic anhydride on an oxygen-precovered surface shows different behavior to that of the clean surface.<sup>9</sup> The anhydride ring opening is accompanied by a reaction with adsorbed oxygen resulting in the formation of a phthalate (dicarboxylate) species.

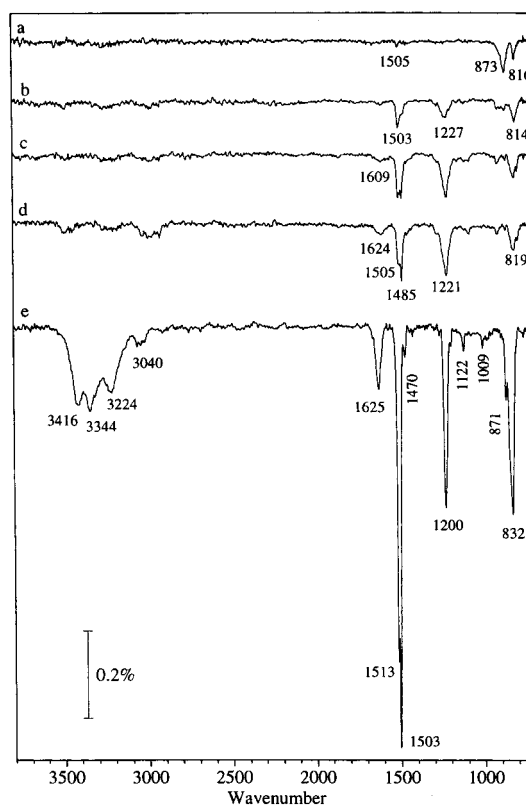


**Figure 7.** IR spectra of ODA adsorption on clean Cu{110} with increasing coverage at 300 K, a–e. Spectrum e corresponds to a multilayer measured at 240 K.

The results for PMDA are in complete agreement with the formation of a similar dicarboxylate species. The new additional modes (cf. Figure 3) at 1553, 1424, and 846  $\text{cm}^{-1}$  are assigned as the carboxylate modes;  $\nu_a(\text{OCO})$ ,  $\nu_s(\text{OCO})$ , and  $\delta(\text{OCO})$ , respectively. Again, only one anhydride group reacts, as the anhydride ring modes of the second unreacted group are clearly evident. Additionally, the symmetric stretching modes are more intense than their asymmetric counterparts which is in agreement with the proposed structure shown in Figure 6.

#### 4. Adsorption of ODA on Clean Cu{110} Surface

The changes in the IR spectra as the clean surface is exposed to a slow continuous dose of ODA at 300 K are shown in spectra a–d of Figure 7. Spectrum e is of a multilayer taken at 200 K which is shown as a comparison to gauge the frequencies and relative intensities of the modes of intact ODA. At 300 K, bands are initially observed at 873, 816  $\text{cm}^{-1}$  and a very small band at 1505  $\text{cm}^{-1}$ . With increasing coverage there is a change in their relative intensity as additional bands appear at 1624, 1505, 1485, 1221, 1100, 922, and 819  $\text{cm}^{-1}$ . The broad features above 3100  $\text{cm}^{-1}$  are difficult to assign with certainty as these can arise from detector ice bands, although in the multilayer there is no ambiguity that these arise from the  $\nu(\text{NH}_2)$  modes. At 300 K, the changes in the spectra again indicate some reorientation of the molecules with increasing coverage. An HREELS spectrum of the saturated surface measured by Plank et al.<sup>15</sup> shows strong similarity to our equivalent IR spectrum. The modes at saturation are assigned as 1624  $\text{cm}^{-1}$   $\delta(\text{NH}_2)$  and  $\nu(\text{C}-\text{C})$ ; 1450–1510  $\text{cm}^{-1}$  aromatic ring stretches; 1270  $\text{cm}^{-1}$   $\nu(\text{C}-\text{N})$  (very weakly observed), 1221  $\nu_a(\text{COC})$ , 922  $\text{cm}^{-1}$   $\nu_s(\text{COC})$ , 800–900  $\text{cm}^{-1}$   $\gamma(\text{CH})$  modes. The changes in the IR spectra with increasing coverage are characteristic of the adsorption of functionalized aromatic molecules. We have

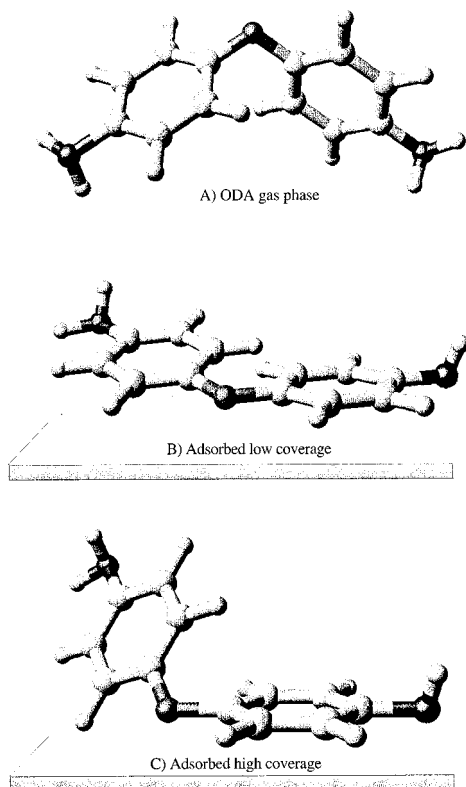


**Figure 8.** Conformation of the gas phase ODA molecule and the ODA-derived species from adsorption onto the clean Cu{110} surface at low and high coverages.

already shown for benzoate,<sup>23</sup> phthalic anhydride,<sup>9</sup> and here PMDA that aromatic molecules on this surface seek to minimize their "footprints" by changing from a parallel to upright geometry with increasing coverage. The ODA molecule is believed to be of  $C_2$  symmetry in the gas phase with the phenyl groups twisted  $+45^\circ$  and  $-45^\circ$  out of the C–O–C plane<sup>10,15</sup> (Figure 8A). This structure of the intact ODA molecule is not consistent with a conformation in which both aromatic rings are parallel to the surface plane. We exclude the possibility of dissociation of the ether link as clearly the  $\nu_s(\text{C–O–C})$  ether mode is observed with increasing coverage. The only other possibility is that the conformation of the molecule changes on adsorption at low coverages, possibly twisting the phenyl groups into the plane of the C–O–C plane to give a more planar geometry (Figure 8b). Any steric strain due to repulsion may be overcome by the increased bonding interaction. At higher coverages, the IR spectra are consistent with the model proposed by Plank et al.<sup>15</sup> with one phenyl group parallel to the surface bonded through the N and the other inclined (Figure 8c). The group parallel to the surface is similar to that from the adsorption of aniline on Cu{110},<sup>24</sup> which leads to the formation of a  $\text{C}_6\text{H}_5\text{NH}$  species bonded through both the N and the aromatic ring. Clearly more work is needed to understand the exact behavior of the ODA molecule on the surface.

## 5. Reaction between Adsorbed PMDA and ODA

**5.1. Results.** The reaction between these two molecules has been studied at room temperature by first adsorbing PMDA onto the surface and exposing the saturated surface to ODA. Although we have shown that a number of different species and orientations can be derived from the adsorption of PMDA onto the clean and oxygen-precovered Cu{110} surface, we restrict our studies to the reaction of saturation coverages on the two

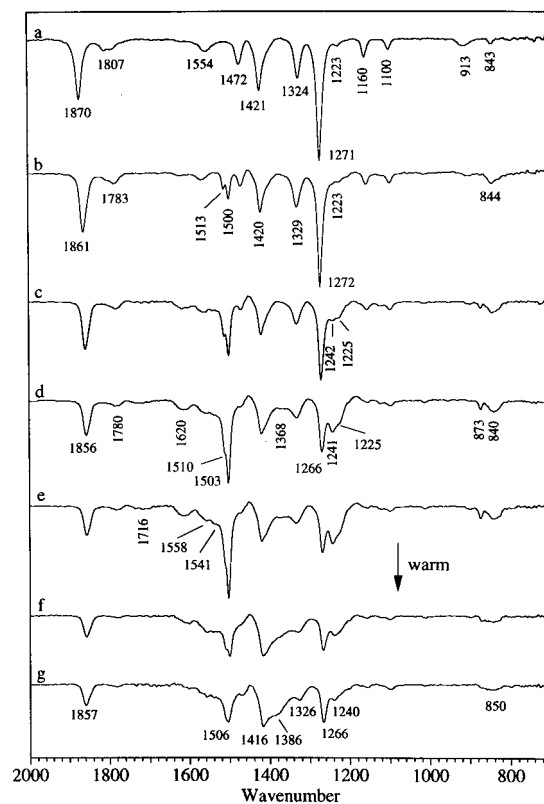


**Figure 9.** IR spectra of PMDA adsorbed on (2×1)O/Cu{110}, spectrum a, subjected to increasing exposure of ODA at 300 K, spectra b–e. Spectra f and g after warming to 410 and 520 K, respectively.

surfaces. The geometry of the dicarboxylate species, formed by PMDA on the oxygen-precovered surface, with its more upright anhydride group and stronger IR bands makes it better suited to follow the reaction. Therefore, we begin with a surface saturated with this species, spectrum a of Figure 9, and follow the changes in the IR spectrum with increasing exposure to ODA. Spectra b–e show the changes in the IR spectrum with increasing exposure of ODA. We note that the flux of ODA used was the same as that for adsorption onto the clean surface shown in Figure 7. Even for the lowest exposure, the appearance of bands at 1513 and 1500  $\text{cm}^{-1}$  shows that ODA is present in the overlayer. These bands continue to grow and, at saturation, spectrum e, additional modes are observed at 1620 and 1242  $\text{cm}^{-1}$ . It is unlikely that these arise from ODA directly adsorbed on the Cu surface, as the surface is already saturated with the dicarboxylate species and the anhydride modes are attenuated. Although the former band can be assigned to the  $\delta(\text{NH}_2)$  mode of ODA, the latter does not correspond to any band of ODA or the adsorbed PMDA. We assign the 1242  $\text{cm}^{-1}$  mode to a  $\nu(\text{CN})$  band associated with a ring-opening reaction resulting in an amic acid species. As this saturated surface is warmed to 410 and 520 K, spectra f and g, changes are observed in the IR spectra. First, there is the attenuation of the modes of the ODA, and more significantly the appearance of a feature around 1386  $\text{cm}^{-1}$ , at 520 K, the temperature where the internal condensation reaction (imidization) of the amic acid starts. However, the formation of an imide has characteristic modes at 1780 and 1730  $\text{cm}^{-1}$ ,<sup>26–29</sup> which are clearly not observed and, therefore, this spectrum does not serve to indicate at this stage the closure of the ring to an imide. We also note that once the surface has been heated to above 520 K and cooled back to room temperature no further changes were observed in the IR spectra with additional exposure of either PMDA or ODA.

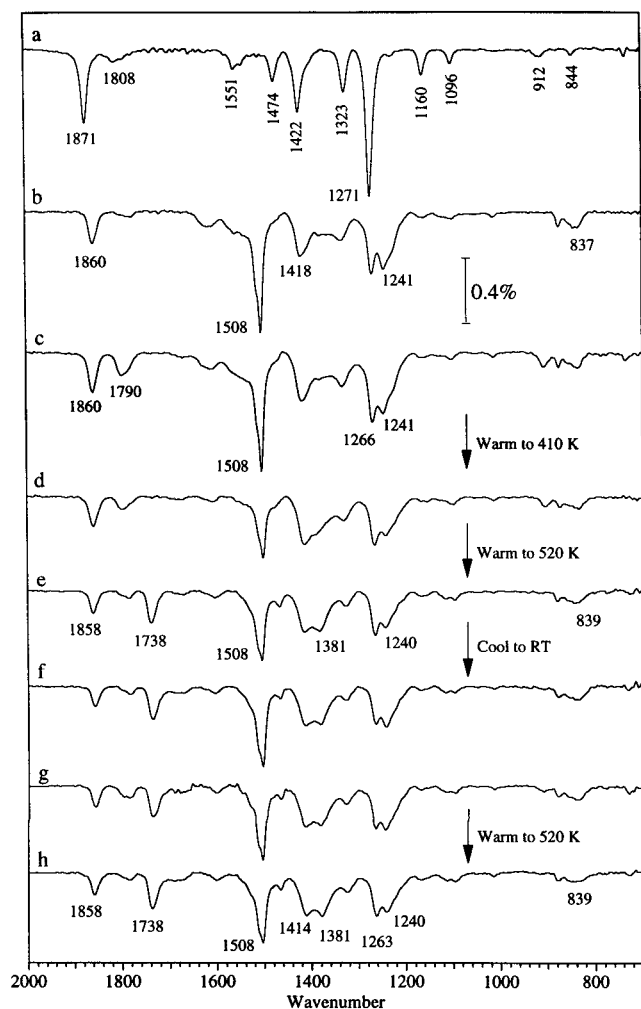


**Figure 10.** IR spectra of PMDA adsorbed on  $(2 \times 1)\text{O}/\text{Cu}\{110\}$ , spectrum a, subjected to saturation exposure of ODA followed by saturation exposure of PMDA at 300 K, spectra b and c. Spectra d and e after warming to 410 and 520 K, respectively. Spectrum f, cool to 300 K and reexpose to ODA, spectrum g reexpose to PMDA, and spectrum h after warming that surface to 520 K.

Although the above spectra clearly indicate a ring-opening reaction at 300 K, the absence of the expected modes which characterize the ring closure process makes it difficult to characterize the surface species. However, the reaction mechanism becomes much clearer when a sequence of spectra are collected in which we begin with a saturated surface with the dicarboxylate species and expose this to ODA exactly as shown above and finally reexpose to PMDA without intermediate heating, spectra a–c of Figure 10. The IR spectra for the initial PMDA/ODA sequence follow those shown above. The additional dose of PMDA shows little change in the IR spectra other than an increase in intensity of the asymmetric PMDA carbonyl mode at  $1790\text{ cm}^{-1}$ . Again as the surface is warmed to 410 K the IR spectra are similar to those shown above. However, this time, as this surface is warmed above 520 K, spectrum e, a new mode is observed at  $1738\text{ cm}^{-1}$ , which is one of the modes most clearly characterizing imidization. Again, on cooling back to 300 K, reexposing to ODA or PMDA, and warming to above 520 K, no further change in the IR spectra, spectra f–h, are observed.

The above spectra show ring-opening and -closing reactions; however, some additional modes which are expected are still absent. A distinct lack of modes is often attributed to either the

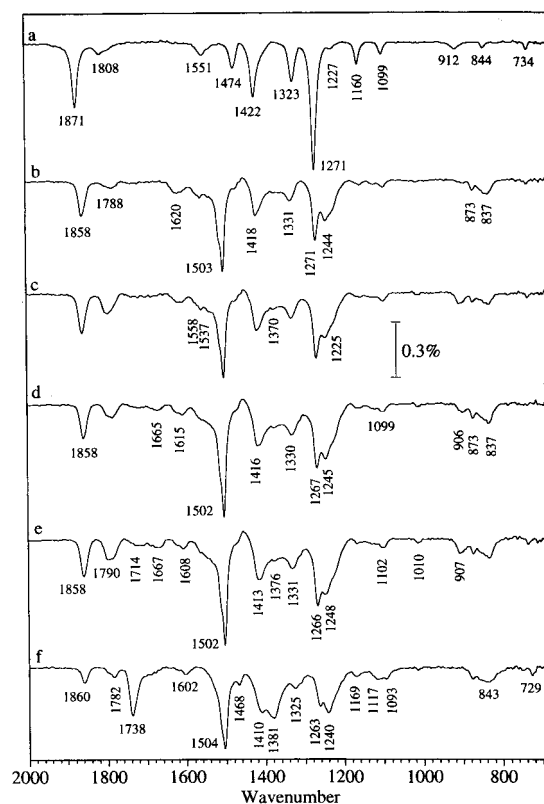


**Figure 11.** IR spectra of PMDA adsorbed on  $(2 \times 1)\text{O}/\text{Cu}\{110\}$ , spectrum a, and successive saturation exposures of ODA, PMDA, ODA, and PMDA at 300 K, spectra b–e respectively. Spectrum f was recorded after warming to 520 K.

orientation or intensity. The intensity problem can be overcome by producing a thick overlayer to see if the expected additional modes appear. Spectra a–e of Figure 11 show the changes in the IR spectra after alternating exposure cycles of PMDA/ODA/PMDA/ODA/PMDA and subsequently heating to 520 K (spectrum f). In this series, spectra d and e show weak broad bands at  $1667$  and  $1714\text{ cm}^{-1}$ . These are expected for the carbonyl groups of the amide and acid groups formed by the ring-opening reaction. Figure 12 is a comparison showing an increase in the intensity of the imide modes at  $1738$  and  $1380\text{ cm}^{-1}$  with increasing PMDA/ODA exposure cycles, indicating an increase in the chain length of the imide oligomers. The band at  $1860\text{ cm}^{-1}$ , characteristic of the anhydride ring, decreases in relative intensity but implies the presence of such rings at the outermost molecular layer available for further reaction.

The results from the reaction sequences starting with the anhydride species formed on the clean  $\text{Cu}\{110\}$  surface show strong similarity to those starting with the phthalate species found on the oxygen-preadsorbed surface, although there is a reduction in the absolute intensities of all the IR bands which we ascribe to the different orientation of the starting species. Figure 13 shows the IR spectra after exposure of the clean  $\text{Cu}\{110\}$  surface to PMDA/ODA/PMDA/ODA and then warming to 410 and 520 K. The results are in good agreement with those expected for a ring-opening and -closing reaction. Although we note that the temperature at which imidization begins may be lower than that found for the phthalate type species as seen from spectrum e of Figure 13 where at 410 K there is already the appearance of a mode at  $1730\text{ cm}^{-1}$ .

**5.2. Discussion.** The IR spectra show that the reaction between PMDA and ODA can be separated into the ring-opening and ring-closing processes, both these can result in at

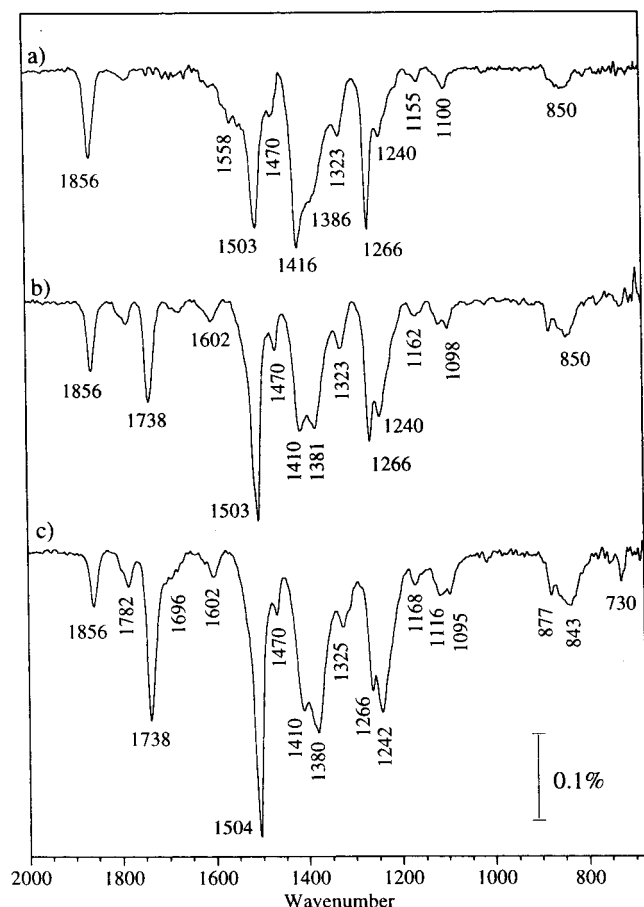


**Figure 12.** Comparison of the imide IR spectra from  $(2 \times 1)O/Cu\{110\}$  after a single PMDA/ODA exposure cycle, spectrum a, spectrum b after a PMDA/ODA/PMDA exposure cycles and spectrum c after PMDA/ODA/PMDA/ODA/PMDA exposure cycles.

least two different species. Figure 14 illustrates these species and the main vibrational modes which characterize them. In principle, it should be relatively straightforward to distinguish between the formation of all the species outlined in Figure 14 from their characteristic group frequencies. Additionally, the relative orientations of each functional group may be deduced by considering the direction of the dynamic dipole associated with the vibrations. However, care has to be taken in interpreting the RAIRS data as the observed intensity for a given mode depends on two factors. First, the dipole selection rule inherent of RAIRS which allows only those vibrations which give a significant dynamic dipole moment directed perpendicular to the surface to be IR active, and second, the intensity of a given mode also depends on the IR absorption cross section for that mode. Generally, the IR transmission spectra of the molecules being studied serve as guide to the relative intensities of the modes. The latter is particularly true for  $\nu(OH)$  which are generally broad and weak and rarely observed in submonolayer concentrations in RAIRS experiments; therefore, we note that we did not observe any bands above  $3100\text{ cm}^{-1}$  that could be associated with either  $\nu(OH)$  or  $\nu(NH)$ : HREELS does show these features.

The initial ring-opening reaction leads to the formation of an amic acid, although the carboxylic acid group of this species can subsequently react with excess ODA to form a salt.<sup>14</sup> In either case, an amide group is produced and has characteristic frequencies of  $1660$ ,  $1540$ , and  $1340\text{ cm}^{-1}$  for  $\nu(C=O)$ ,  $\delta(NH)$ , and  $\nu(CN)$ , respectively. On initial inspection, the IR spectra from an anhydride-terminated surface exposed to ODA (Figure

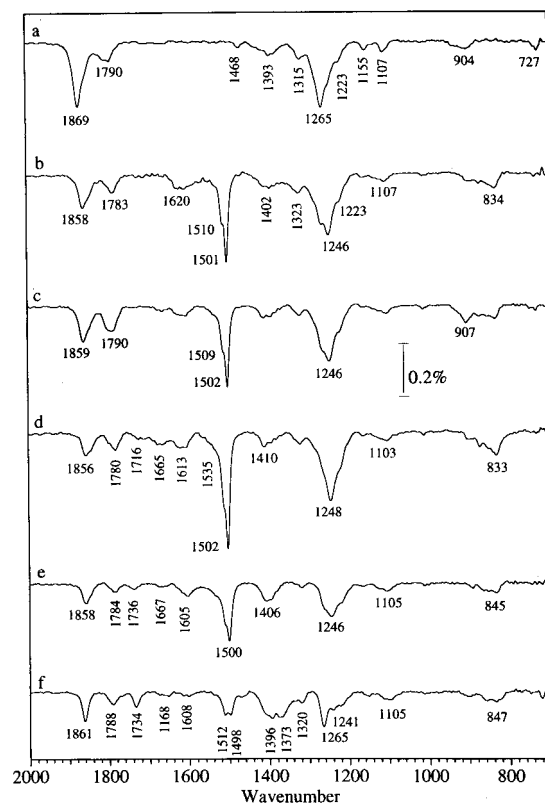


**Figure 13.** IR spectra of PMDA adsorbed on clean  $Cu\{110\}$ , spectrum a. Spectra b–d taken during continual slow ODA exposure at  $300\text{ K}$ . Spectrum e and f after warming to  $410$  and  $520\text{ K}$ , respectively.

Anhydride	Amic Acid	Salt	Isolmide	Imide
$\nu_s(C=O)$ 1860 $\nu_a(C=O)$ 1780 $\nu_s(COC)$ 1260 $\nu_a(COC)$ 920	$\nu_{acid}(C=O)$ 1710 $\nu_{amide}(C=O)$ 1660 $\nu_{acid}(C-O)$ 1260 $\delta_{amide}(NH)$ 1540	$\nu_s(OCO)$ 1600 $\nu_a(OCO)$ 1420 $\nu_{amide}(CO)$ 1660 $\delta_{amide}(NH)$ 1540	$\nu(C=O)$ 1800 $\nu(C=N)$ 1710 $\nu_s(COC)$ 1260 $\nu_a(COC)$ 920	$\nu_s(C=O)$ 1780 $\nu_a(C=O)$ 1730 $\nu_s(CNC)$ 1370 $\nu_a(CNC)$ 1135

**Figure 14.** Illustration of key reaction products and the main group frequencies ( $\text{cm}^{-1}$ ) that identify them.

9) do not appear to show these bands with any significant intensity, although at saturation two of these appear as very weak bands at  $1541$  and  $1368\text{ cm}^{-1}$ . These bands are found to be relatively strong in the amic acid therefore the relatively weak intensity in these experiment may arise from the orientation of these groups. The band associated with the acid group are expected at  $\nu(C=O)$   $1717\text{ cm}^{-1}$ ,  $\nu(C-O)$   $1303\text{ cm}^{-1}$ , and  $\delta(C-O-H)$   $1407\text{ cm}^{-1}$ . Again, these do not appear as distinct modes with any significant intensity, although at saturation the  $\nu(C=O)$  is seen as a very weak broad band at  $1716\text{ cm}^{-1}$ . However, the modes expected for both the amide and the acid groups become more clear when a number of PMDA/ODA adsorption cycles are performed, as can be seen from spectrum e of Figure 11. The weakness of these modes, together with the fact that there is overlap of modes from the acid and the salt, makes the identification of the species from which they arise difficult. The formation of the salt is believed to prevent imidization, which suggests that primarily acid rather than salt groups are present since imidization is clearly observed.

On warming, the surface after one PMDA/ODA cycle to  $410\text{ K}$ , spectrum f of Figure 9, changes in the spectra are already observed with the attenuation of all the modes except



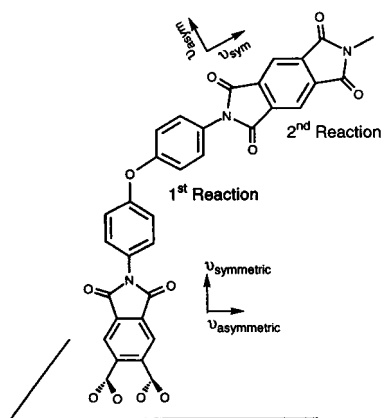


**Figure 15.** Illustration of imide reaction product after PMDA/ODA/PMDA exposure cycle on (2×1)O/Cu{110} surface. Also shown is the direction of the dynamic dipole of the symmetric and asymmetric stretching modes of the imide after the first and second reactions.

the  $\nu(\text{OCO})$  at  $1416\text{ cm}^{-1}$ . We do not observe any desorption in the mass spectrum at this stage; however, on warming to above 470 K, desorption of water was clearly seen. This is accompanied by a further subtle change in the IR spectrum with the appearance of a band at  $1386\text{ cm}^{-1}$ . The evolution of water is consistent with the ring closure process. The IR spectrum does not appear to show the expected structure associated with imidization, as the main  $\nu(\text{C=O})$  modes of an imide are expected at  $1780$  and  $1730\text{ cm}^{-1}$ . The observation of these modes depends on their orientation with respect to the surface and also with their IR absorption strengths. Both transmission IR and RAIR studies of thin polyimide films show that the asymmetric imide  $\nu(\text{C=O})$  at  $1730\text{ cm}^{-1}$  is more than a factor of 10 more intense than its counterpart symmetric  $\nu(\text{C=O})$  at  $1780\text{ cm}^{-1}$ .<sup>26–28</sup> This suggests that these modes may not be suitable to measure the orientation and onset of the polymerization sequence. There is, however, another mode of the same symmetry characteristic of the imidization which has a larger intensity, the axial  $\nu(\text{CNC})$  at  $1378\text{ cm}^{-1}$ . Therefore, the appearance of this mode with heating suggests that imidization has occurred, and the absence of the symmetric  $\nu(\text{C=O})$  of the imide is rather due to its low IR absorption coefficient. Figure 15 shows a schematic of the start of a polymerization sequence together with the direction the dipoles of the symmetric and asymmetric stretching modes of the imide functional groups. From this, the observation of the imide mode at  $1730\text{ cm}^{-1}$  only after the second dose of PMDA also becomes clear as the dynamic dipole associated with this mode in the first coupling step is parallel to the surface and only in later steps does it become more perpendicular to the surface. In the thicker films, the relative intensity of the  $1780$  and  $1730\text{ cm}^{-1}$  modes suggest the C–N axis of the imide groups is inclined at  $45^\circ$  to the surface.

One intriguing and unresolved result of this study is that, after curing, further reaction is not observed regardless of the surface termination with amine or anhydride groups, under the conditions used in this study, although the growth of modes of polyimide with increasing number of PMDA/ODA cycles before curing suggests that polymer chains increase in size. Under the conditions used in this study with low-pressure deposition for both molecules, the efficiency of the reaction to the amic acid suggests a high reaction probability, the reaction probability being the likelihood for an incoming molecule to react at a surface as opposed to being reflected back into the gas phase. It should be noted that the reaction probability at a surface is a complex function, depending on the orientation and residence

times of the incoming molecules. A decrease in the reaction probability after curing may account for the observation but must depend on significant structural and/or chemical changes at the surface. Some support for this argument comes from the fact that we have attempted to observe the anhydride ring-opening process at room temperature with aniline without success even with pressures of aniline as high as  $1 \times 10^{-6}$  mbar. However, in our previous HREELS study it was found that a reaction could be observed if the aniline was dosed at low temperature and then warmed to room temperature to form the amic acid.<sup>6</sup> Parallel studies with HREELS on silicon show similar results with aniline/PMDA, although the reaction with phenyl diamine/PMDA is more analogous to that with ODA. An alternative explanation for the lack of reactivity after curing may be cross-linking of the terminal groups with neighboring molecules therefore making the surface of the polymer inert to further reaction.

## 6. Conclusion

The objective of this study was to construct and characterize an oligimide in a layer by layer manner, thus avoiding any excess of either of the monomers, in contrast to previous methods which have relied on codeposition. In the process, we have characterized the adsorption of PMDA and ODA on Cu-(110) as a function of temperature and coverage. The adsorption of PMDA on oxygen predosed Cu(110) has also been characterized. Orientation of the PMDA/ODA oligomer is more nearly perpendicular to the surface if a preadsorbed oxygen surface is used to initiate the growth. Curing the surface between deposition cycles leads to an inert surface which inhibits further growth. Longer oligomer sequences are best obtained by deposition sequences at room temperature with imidization only as the final step.

**Acknowledgment.** EPSRC is acknowledged for an equipment grant and a research fellowship for S.H. We also thank B. G. Frederick and T. Bitzer for helpful discussions.

## References and Notes

- (1) Gosh, M. K.; Mittal, K. L., Eds. *Polyimides: Fundamental Aspects and Technological Applications*; Marcel Dekker: New York, 1993.
- (2) Sroog, C. E. *J. Polym. Sci. Macromol. Rev.* **1976**, *11*, 161.
- (3) Salem, J. R.; Sequeda, F. O.; Duran, J.; Lee, W. Y.; Yang, R. M. *J. Vac. Sci. Technol.* **1986**, *A4*, 369.
- (4) Yoshimura, T.; Tatsura, S.; Sotoyama, W. *Appl. Phys. Lett.* **1991**, *59*, 482.
- (5) Richardson, N. V.; Frederick, B. G.; Unertl, W. N.; Farrash, A. *EL. Surf. Sci.* **1994**, *309*, 124.
- (6) Frederick, B. G.; Richardson, N. V.; Unertl, W. N.; Farrash, A. *EL. Surf. Interface Anal.* **1993**, *20*, 434.
- (7) Bitzer, T.; Richardson, N. V. *Appl. Phys. Lett.* **1997**, *71*, 662.
- (8) Frederick, B. G.; Ashton, M. R.; Richardson, N. V.; Jones, T. S. *Surf. Sci.* **1993**, *292*, 33.
- (9) Haq, S.; Bainbridge, R. C.; Frederick, B. G.; Richardson, N. V. Submitted for publication in *J. Phys. Chem.*
- (10) Hahn, C.; Strunskus, T.; Frankel, D.; Grunze, M. *J. Electron Spectrosc. Relat. Phenom.* **1990**, *54/55*, 1123.
- (11) Child, C. M.; Fieberg, J. E.; Campion, A. *Surf. Sci.* **1997**, *372*, L254. [12] Takahashi, Y.; Iijima, M.; Inagawa, K.; Itoh, A. *J. Vac. Sci. Technol.* **1987**, *A5* (4), 2253.
- (12) Lamb, R. N.; Grunze, M. *Surf. Sci.* **1988**, *204*, 183.
- (13) Dimitrakopoulos, C. D.; Machin, E. S.; Kowalczyk, S. P. *Macromolecules* **1996**, *29*, 5818.
- (14) Plank, R. V.; DiNardo, N. J.; Vohs, J. M. *J. Vac. Sci. Technol. A* **1996**, *14*(6), 3174.
- (15) Hahn, C.; Strunskus, T.; Grunze, M. *J. Phys. Chem.* **1994**, *98*, 3851.
- (16) Boeyens, C. A.; Herbstein, F. H. *J. Phys. Chem.* **1965**, *69*, 2160.
- (17) Ashton, M. R.; Jones, T. S.; Richardson, N. V.; Mack, R. G.; Unertl, W. N. *J. Elec. Spec. Rel. Phenom.* **1990**, *54/55*, 1133.
- (18) Perry, S. S.; Campion, A. *Surf. Sci.* **1990**, *234*, L275.

- (19) Meyer, W.; Grunze, M.; Lamb, R.; Ortega-Vilamil, A.; Schrepp, W. Braun, W. *Surf. Sci.* **1992**, 273, 205.
- (20) Ivanecky, J.E., III; Child, C.M. Campion, A. *Surf. Sci.* **1995**, 325, L428.
- (21) Perry, S. S.; Campion, A. *Surf. Sci.* **1991**, 259, 207.
- (22) Frederick, B. G.; Leibsle, F. M.; Haq, S.; Richardson, N. V. *Surf. Rev. Lett.* **1996**, 3, 1523.
- (23) Plank, R. V.; DiNardo, N. J.; Vohs, J. M. *Surf. Sci.* **1995**, 340, L971.
- (24) Hase, Y.; Kawai, K.; Sala, O. *J. Mol. Struct.* **1975**, 26, 297.
- (25) Ishida, H.; Wellinghoff, S. T.; Baer, E.; Koenig, J. L. *Macromolecules* **1980**, 13, 826.
- (26) Young, J. T.; Tsai, W. H.; Boerio, F. J. *Macromolecules* **1992**, 25, 887.
- (27) Burrell, M. C.; Codella, P. J.; Fontana, J. A.; Chera, J. J.; McConnell, M. D. *J. Vac. Sci. Technol. A* **1989**, 7(1), 55.
- (28) Snyder, R. W.; Thomson, B.; Bartges, B.; Czerniaski, D.; Painter, P. C. *Macromolecules* **1989**, 22, 4166.